eXPRESS Polymer Letters Vol.5, No.4 (2011) 308–317
Available online at www.expresspolymlett.com
DOI: 10.3144/expresspolymlett.2011.31

Fabrication of electrospun polyacrylonitrile ion-exchange membranes for application in lysozym

H. T. Chiu[1*], *J. M. Lin*[1], *T. H. Cheng*[2], *S. Y. Chou*[2]

[1]Department of Materials Science and Engineering National Taiwan University of Science and Technology, No.43, Keelung Rd., Section 4, Taipei, Taiwan
[2]Department of Products, Taiwan Textile Research Institute, No. 6, Chengtian Rd., Tucheng City, Taipei County 23674, Taiwan

Received 18 August 2010; accepted in revised form 7 November 2010

Abstract. Ion exchange (IEX) chromatography is commonly used in separation and purification systems. However, micropore blockage within its resin structure can easily lead to a reduction in the effectiveness of purification. To tackle this problem, we adopted the concept of membrane separation by combining electrospinning techniques with rapid alkaline hydrolysis to prepare a weak acid IEX nanofibrous membrane (AEA-COOH), consisting of polyethyleneterephthalate (PET) meltblown fabric as a supporting layer, with upper and lower IEX layers consisting of polyacrylonitrile (PAN) nanofibrous membranes. To determine the characteristics of the AEA-COOH membrane, we used the commercial product Sartobind® C IEX membrane as the standard of comparison. Results showed that the base weight and thickness of AEA-COOH were 33 and 64%, relative to Sartobind® C membrane. The thermo-degradable temperature of AEA-COOH membrane (320°C) was far higher than that of Sartobind® C (115°C), indicating high thermal stability. Finally, comparisons between the lysozyme adsorption rates and capacity of various IEX membranes confirmed that AEA-COOH was lighter, thinner, faster, possessing higher protein adsorption efficiency than Sartobind® C membrane.

Keywords: *polymer membranes, electrospun, nanofiber, ion-exchange, lysozymes adsorption*

1. Introduction

A conventional ion exchange resin usually has a gel or granular structure, composed of styrene or acrylic material [1]. However, micropore structures within the resin result in lower molecular adsorption/desorption rates, due to diffusion distance. With an increase in the pace of processing, the volume of adsorbed molecules increased, and an increase in the frequency of its application rapidly decreased the efficiency of its ion exchange capability, to the point where it was suitable only for smaller molecules. In addition, micropores in traditional resins are easily blocked, which reduces the effectiveness of purification and decreases the regeneration response rate. Furthermore, the resin itself is vulnerable to damage due to pressure [2–3]. To tackle the above problems, the fiber structure of the ion exchange filters has undergone significant development in recent years. Compared to resins of other types of gel or granular structure, fiber structured resins are simple to use, thanks to their large surface area, and possess high adsorption capacity, fast ion exchange and regeneration rate, as well as other unique features [4–6]. It is widely used in dyes, precious metals, protein pharmaceuticals and other high value-added materials during the enrichment and purification; it is also used in wastewater and gas decontamination processes. The potential benefits and value to researchers cannot be overlooked [7–11].

*Corresponding author, e-mail: hchiu@mail.ntust.edu.tw

According to previous studies [12–18], electrospinning is the only direct, efficient, and continuous method for producing polymer nanofibers showing the most promise and greatest efficiency. Hundreds of polymer nanofibers of various kinds have been developed using electrospinning. Electrospinning polymer processing systems deliver polymer solutions to a spin feeder, to form liquid droplets. With the application of a high voltage charge, the electrical charge within the polymer mutually excludes and overcomes the surface tension of the solution. The surface of the droplets spray a charged liquid column, which, under the continuous effect of the electric field, quickly spiral downward to form a lashing extension. The resulting nanofiber is a thousand times thinner than fibers manufactured using normal micro-spinning technology. As the process continues, the solvent in the solution rapidly evaporates. Finally, non-woven membranes of nanometer fiber diameter are collected in the collector plate beneath. By electrospinning, fibers with a diameter between a few dozen to several hundred nanometers could be manufactured. When compared to traditional fibers (diameter of 50 microns) under the same volumetric conditions, these fibers had a smaller diameter pore aperture, more densely interconnected pores and increased porosity. In addition, the specific surface area of nanofibers is approximately 100 times that of normal fibers. Thus, nanofiber membrane filters, when compared to traditional filters, have a higher throughput, lower loss, lower energy consumption, shorter transmission distance, higher adsorption, faster reaction, as well as other advantages [19–21].

Polyacrylonitrile (PAN) possesses high mechanical strength thanks to the strong hydrogen bonding of its molecular structure. It also exhibits strong chemical resistance, excellent acid-proof alkalinity, resistance to sunlight, a diminished susceptibility to humidity, and low cost [22–23]. Thus, it has caught the attention of many researchers, in the past 10 years. It is widely used in the preparation of microfiltration (MF), ultrafiltration (UF) and hollow fiber membranes [24–26]. In addition, PAN molecular chains carry a cyano group, which can be modified. It is hydrolysable and can be adjusted to achieve functionality in a number of applications. If part of the hydrolysis process could be performed with carboxyl functional groups (–COOH) in a solution, it could quickly adsorb metal ions, lysozymes, and other molecules. Its unique features include high absorption capacity, fast absorption speed, and good dynamic performance. It is an excellent material for use in the purification of heavy metal wastewater and lysozymes [27–30].

In this study, we first used electrospinning technology to prepare PAN/PET/PAN nanofiber composite membrane. The nanofiber was stacked into a 3D reticular fiber structure through cross laying. This gave the membrane a high specific surface area, higher porosity (>80%), and micron size membrane pores. With the use of alkaline hydrolysis techniques, high-density carboxyl groups appeared on the surface of PAN nanofibers. This prepared the nanofiber membrane for weak acid ion exchange. During the exchange of ions through the nanofiber membrane shortened the distance in molecular diffusion, thereby accelerating the rate of ion exchange and improving adsorption capacity. Scanning electron microscopy, porosity analysis, and Toluidine Blue O (TBO) functional groups detector were used to analyze micro-porous PAN/PET/PAN structure, patterns, pore size, distribution, and density of nanofiber composite membrane and its functional groups. Finally, the nanofiber composite membrane was compared to commercial product Sartobind® C membrane in order to further explore the different ion exchange membranes in the lysozyme adsorption.

2. Experiments

2.1. Materials

Polyacrylonitrile (PAN) yarn (M_w = 120 000, containing 93% acrylonitrile and 7% vinylacetate) and dimethylacetamide (DMAc) were purchased from Fortune Industries Inc (Tao-Yuan, Taiwan) and I-Chang Chemical Co., Ltd (Taipei, Taiwan), respectively. Sodium hydroxide (NaOH) was from J.T. Baker. Lysozyme and Toluidine Blue O (TBO) were from Sigma. The reagents and solvents were of analytical grade and used without further purification.

2.2. Electrospinning of polyacrylonitrile

Electrospinning device was purchased from Jyi Goang Enterprise Co., Ltd. (Taipei, Taiwan). PAN yarn was dissolved in DMAc at a concentration of 15% (w/v). PAN/DMAc solution was loaded into a

syringe and delivered to the tip of a 21-gauge stainless steel nozzle with a syringe pump. The nozzle was connected to a power supply and charged to 26.5 kV. The electrospinning mats were collected on nonwoven PET (basis weight 15 g/m^2) and wrapped on a grounded steel sheet. The distance between the tip of the nozzle and the substrate was 15.8 cm, the flow rate was 1ml/h, and the collector rotation rate was 24 cm/s. The nozzle was moving along the y-axis (20 cm), and the frequency was 12 times/min.

2.3. Introduction of anionic moieties into PAN nanofiber membranes

Electrospun PAN nanofiber mats were chemically activated by substituting the nitrile groups with anion carboxylic acid groups as an ion exchange material. First, PAN nanofiber mats were alkaline hydrolyzed by immersion in various concentrations (1N, 2N, 3N) of sodium hydroxide stirred (150 rpm) at different temperatures (25–85°C) for 0–40 min. They were washed out with deionized water until no change in pH was apparent. Finally, the carboxylated electrospun PAN nanofiber mat was treated with 0.1M HCl, followed by drying in an oven, at 60°C.

2.4. Characterization of fabrics

The morphology and diameter of electrospun PAN nanofiber mats before and after the introduction of the ion-exchange groups were observed using a scanning electron microscope (SEM, JEOL, and JSM 6510). All samples were sputter-coated with Pt.

Thermogravimetric analysis (TGA) was conducted with TGA Q50 from TA Instruments at a heating rate of 20°C/min under nitrogen. To characterize the crystallinity of the fibers, wide-angle X-ray diffraction (WAXD, SIEMENS, and D5005) patterns of PAN nanofiber membranes under various alkaline hydrolysis conditions were obtained using an X-ray goniometer operating at 40 kV and 30 mA with a scanning speed of 1°/min.

The distribution of pore size and the mean pore size of electrospun PAN nanofiber mats were determined with a measuring instrument (Perm-Porometer, PMI, USA). The porosity and the specific surface area were measured with fully automatic density analyzer (AccuPyc 1330 Pycnometer) and BET apparatus (Micrometritics, ASPS 2000), respectively.

2.5. Adsorption behavior [31–32]

Subsequent to alkaline hydrolysis, the concentration of carboxyl group on the surface of the PAN nanofiber was measured using Toluidine Blue O (TBO) dye. We placed the modified PAN nanofiber membrane in 2 ml 1mM TBO dyeing agent (dissolved in 1 mM NaOH solution, pH = 10), at room temperature for 6 hours. It was cleaned several times with de-ionized water. This was followed by additional cleaning of the membrane using 0.1 mM NaOH to remove TBO dye adsorbed on the surface of the membrane. Then, 2 ml of 50% acetic acid solution was added to remove the TBO dye of carboxyl ionic bond. Finally, UV spectrum absorption was set to a wavelength of 633 nm for quantitative analysis. Using TBO/COOH = 1:1, the number of carboxyl groups on the membrane surface was calculated. Under lysozyme adsorption conditions, in various time frames, at 298 K, with stirring speed of 150 rpm, the lysozyme initial concentration was 0.5 mg/ml (in 20 mM glycine buffer (pH 9)), and the 595 nm absorbance wavelength was measured using Bio-Rad lysozyme concentration analysis. By using the standard concentration curve of lysozyme, the adsorption capacity of lysozyme nanofiber could be obtained.

3. Results and discussion

3.1. Polyacrylonitrile (PAN) nanofiber membranes

This study combines electrospinning nanofibers with rapid alkaline hydrolysis technology, to develop an ion-exchange nanofiber membrane with high

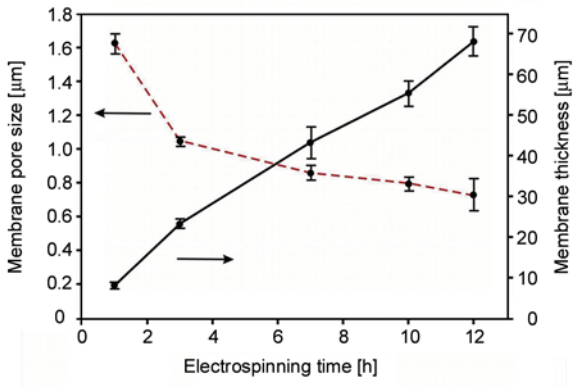

Figure 1. Effect of electrospinning duration on pore size and thickness of PAN nanofiber membranes

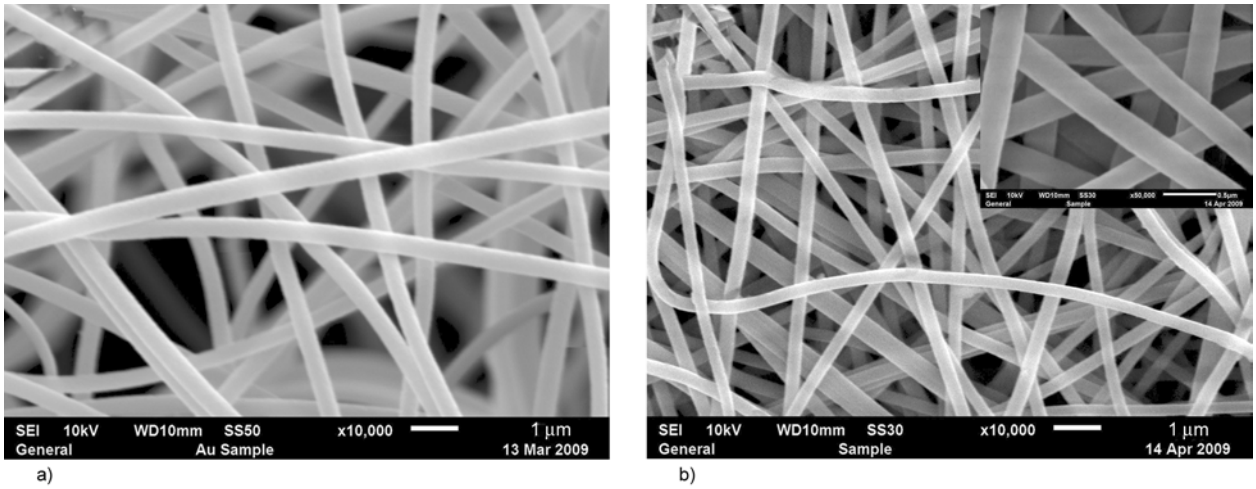

Figure 2. SEM images of electrospun fibers of polyacrylonitrile: (a) electrospinning a PAN nanofiber mat; (b) compacting the mat to increase the volume density of fibers. The insert shows the morphology of nanofibers at a magnification of 50 000.

surface area and high porosity. Figure 1 shows the relationship between the duration of electrospinning and the thickness and average pore size of the electrospun PAN nanofiber membrane. These results indicated that the thickness of nanofiber membrane increased linearly and proportionally to increases in electrospinning duration. Conversely, the average pore diameter declined rapidly over time within the 1–3 h of the spinning time frame, whereupon it was stabilized. The duration of the electrospinning had no significant effect on the pore size of membranes. SEM photos in Figure 2 show electrospun PAN membrane with a loose structure comprising a mat of network of cross-laid nanofibers, with large diametric pores between the fibers. After the heat pressing process, the structure of the membrane increased in density, with an increased in the concentration and distribution of pores. Figure 2b illustrates that variations in the diameter distribution of the PAN nanofiber was uniform, with the average diameter falling between 200–250 nm. Therefore, we selected a PAN nanofiber membrane (thickness: 55.26±2.87 µm, an average pore size: 0.79±0.04 µm), electrospun over a 10 hr period, to serve as the basis for ion-exchange membrane.

3.2. Alkaline hydrolysis of polyacrylonitrile (PAN) nanofiber membranes

Partial hydrolysis is one of the most commonly used methods for PAN-based membranes in the substitution of nitrile groups (–C≡N) with carboxylic acid groups (–COOH) subject to base conditions. The chemical mechanism of alkali hydrolysis reaction is described in detail by Wang *et al.* [27] We used NaOH to quickly and easily alkaline hydrolyze –C≡N bond on the surface of the PAN nanofiber, converting it into COOH functional groups. Figure 3 shows the effects of alkaline hydrolysis on the surface density of COOH PAN nanofibers. Under conditions of fixed alkalization time (10 min) and temperature (25, 40, 55, 70, 85°C), the density of COOH increased, following an increase in the concentration of alkaline hydrolyzed NaOH. The trend of increasing became clear as the temperature of the alkalization increased. When the concentration of NaOH had reached 3N, the COOH density on the PAN nanofiber surface showed the most significant increase.

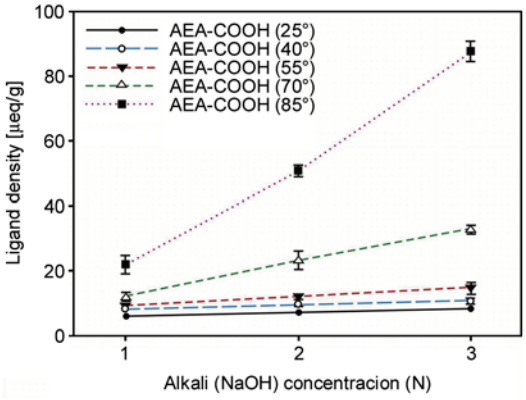

Figure 3. Effect of alkali (NaOH) concentration (N) on carboxylic acid ligand density of AEA-COOH composite membranes

Figure 4 shows the effect of NaOH alkaline hydrolysis temperature on COOH density of the surface of

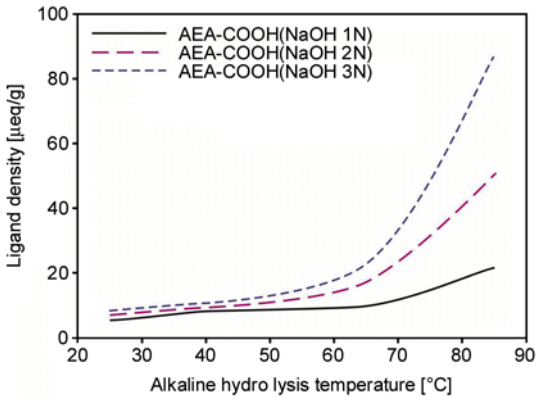

Figure 4. Effect of alkaline hydrolysis temperature on carboxylic acid ligand density of AEA-COOH composite membranes

PAN nanofiber. Under conditions of fixed alkalization time (10 min) and concentration (1N, 2N, 3N), COOH density following an increase in temperature to above 60°C in the alkaline hydrolyzed NaOH. Particularly with a high concentration of NaOH lye, the rate of increase became even more apparent. In addition, the curves in Figure 4 show a critical alkaline hydrolysis temperature in AEA-COOH composite nanofiber membrane. When that temperature was below 60°C, this had little effect on the density of the functional group, but when it increased to above 60°C, COOH the density increased exponentially as a function of temperature.

By TBO dye test analysis, the set COOH density in commercial standard Sartobind® C membrane was determined to be 135.1 μeq/g. Figure 5 shows the effect of NaOH alkaline hydrolysis duration on the COOH density of the PAN nanofiber surface. Under fixed alkalization temperature (85°C) and concentration (3N), when alkaline hydrolysis time for AEA-COOH composite nanofiber membrane was less than 13 minutes, the COOH group density was less than Sartobind® C. However, with a further increase in alkaline hydrolysis duration, PAN nanofiber surface density of COOH groups rapidly increased after 35 minutes. The density of the ionic group was 3.3 times that of the commercial product. After alkaline hydrolysis had continued for more than 60 minutes, the COOH density decreased rapidly to about 1.9 μeq/g. This was due to an overreaction in the hydrolysis reaction, resulting in alkali-soluble conditions in PAN nanofiber (data not shown). Thus, under appropriate reaction conditions, and as the need arose, the density of the functional group AEA-COOH composite nanofiber membrane was modified in order to adjust the duration of alkaline hydrolysis. Yet if Sartobind® C membranes were processed through phase separation, their functional group density could not be adjusted for time, and its operating flexibility was thus limited.

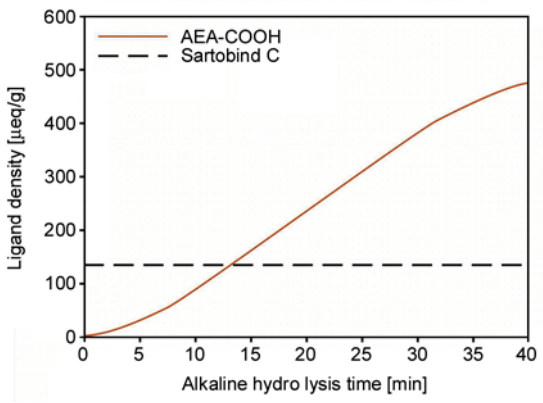

Figure 5. Effect of alkaline hydrolysis time on carboxylic acid ligand density in AEA-COOH composite membranes

3.3. Physical properties of different ion-exchange membranes

Different SEM microstructures of ion exchange membrane are shown in Figure 6. Due to the phase separation process, the surface of the Sartobind® C membrane had an uneven pore distribution; most of the surface area of the membranes was occupied by polymer. Observed by a SEM cross-section view, the Sartobind® C membrane was found to possess an asymmetric structure, which increased its liquid circulation. In this study, the weak acid ion exchange membrane was prepared by electrospinning of PAN nanofiber membrane using NaOH alkaline hydrolysis. Under conditions of fixed alkalization temperature (85°C), concentration (3N), and time (35 min), the membranes were able to maintain the integrity of its nanofiber structure; its surface pore distribution was uniform and dense. With PET serving as an intermediate substrate, it was synthesized into a PAN-PET-PAN (AEA-COOH) asymmetric membrane structure.

Results from PMI pore data test on different membranes showed the relationship between pore distribution [%] and size [μm], as shown in Figure 7. The data confirmed that the pore size distribution on commercial product Sartobind® C membranes was very broad, and its distribution ranged widely from 0.5 to 2.5 μm. The PAN-PET, PAN-PET-PAN ion-

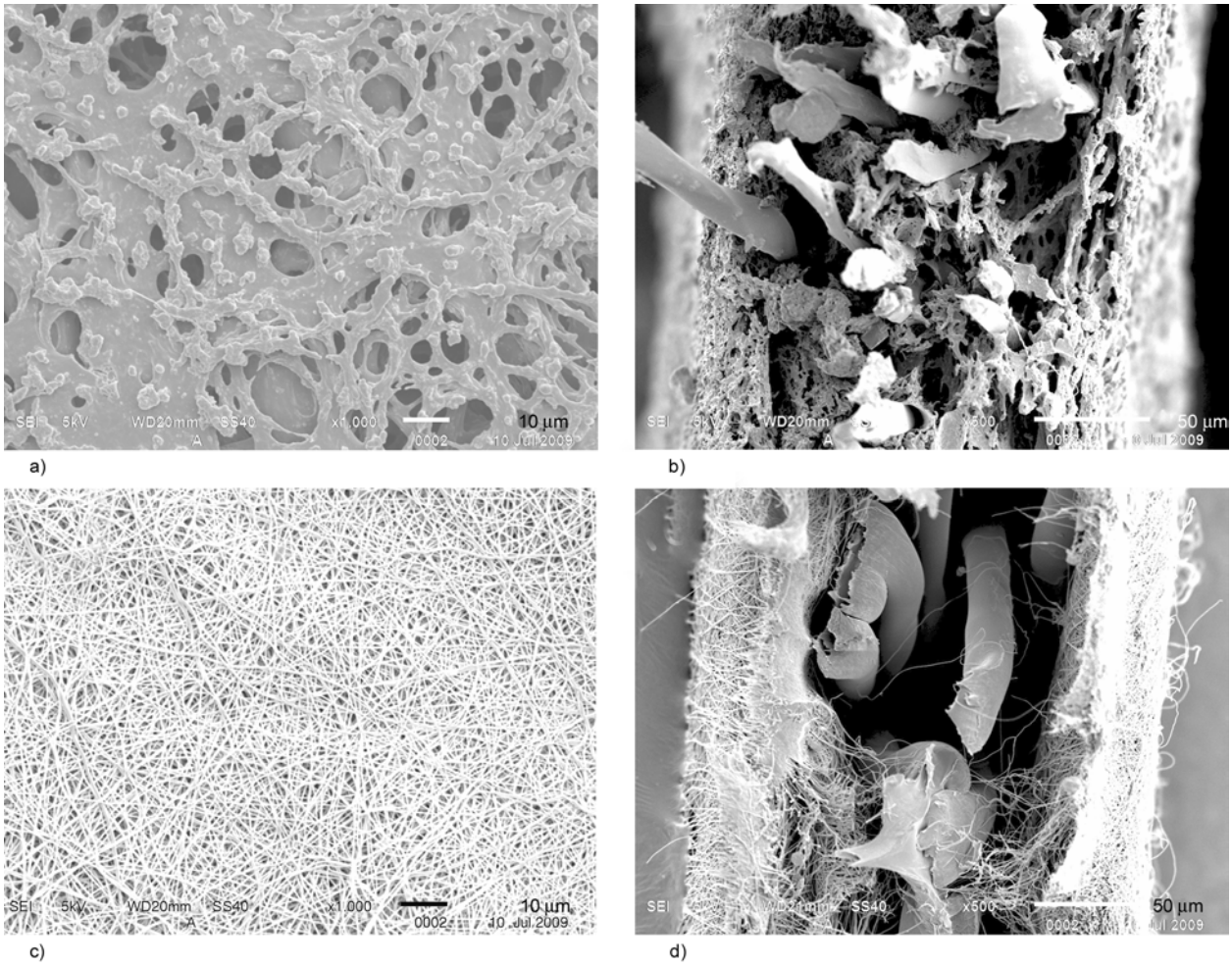

Figure 6. SEM micrographs of ion-exchange membranes. (a) and (b) are surface and cross-sectional images of Sartorius weak acidic cation exchanger (Sartobind® C). (c) and (d) are surface and cross-sectional SEM images of electrospun polyacrylonitrile composite membrane hydrolyzed with NaOH (AEA-COOH).

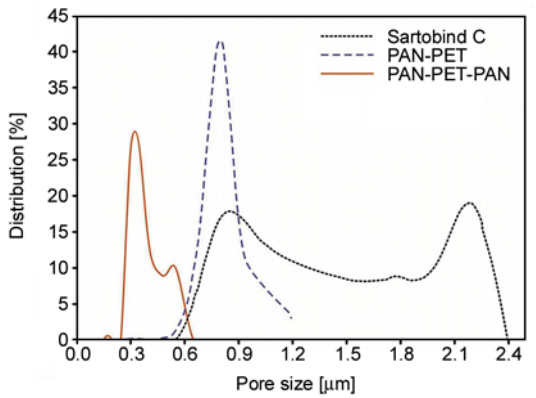

Figure 7. Pore size distribution [%] of different ion-exchange membranes

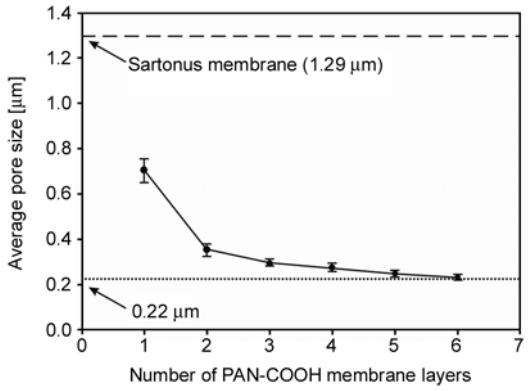

Figure 8. The relationship between average pore size and number of PAN-COOH membrane layers

exchange composite membranes, with their cross-laid, densely packed nanofiber mesh pattern, had a more concentrated arrangement of their pore size and distribution than Sartobind® C membrane.

Figure 8 shows the relationship between the number of PAN-COOH membrane layers and its average pore size; it was similar to control group Sartobind® C membrane in its average pore size of 1.29±0.04 µm. A single PAN-COOH layer combined with PET composite membrane had an average pore size of 0.70±0.05 µm. However, following an increase in the number of PAN-COOH layers,

the average pole diameter quickly declined. When the membrane was in the form of PAN-PET-PAN (PAN-COOH layer number was 2), with an average pore size of 0.36±0.03 μm (less than 0.45 μm); the membrane was capable of micro-filtration. A further increase in the number of layers generated little additional change in the margin of decrease of average pore diameter. However, when the membrane was PAN3-PET-PAN3 (number of PAN-COOH layer was 6), the average pore size was approximately 0.22 μm; the membrane was capable of bacteria filtration. Integrating together all the results from the above experiment showed that, in terms of biotechnology and food purification applications, commercial product Sartobind® C membrane was only capable of ion exchange; its discharged solution still required sterilization, filtration, and other steps in order to complete the purification process. In this study, the capabilities of AEA-COOH nanofiber membrane functional included adsorption, micro-filtration, and bacteria filtration. It could also filter out bacteria and small particles during ion exchange, which reduced the subsequent processing steps and overall purification time.

Table 1 show a comparison between various physical properties of the ion exchange membranes. The result indicated that AEA-COOH membrane's base weight and thickness were approximately 33% and 64% that of Sartobind® C membrane, respectively. In addition, it was discovered, using a BET true density meter, that the AEA-COOH membrane specific surface area (6.1768 m^2/g) was 7 times greater than that of Sartobind® C membrane (0.8873 m^2/g); the ionic base group density was 3.3 times higher, and its porosity (84.4%) was also higher than Sartobind® C membrane (73.4%). These result confirmed that ion exchange membrane formed by PAN nanofibers, was lighter and thinner, with a faster absorption rate and higher volume of liquid circulation than that of Sartobind® C membrane.

Thermal stability analysis of different membranes (e.g. Figure 9 below) showed that the unmodified PAN nanofiber membrane started to thermally decompose at temperatures of about 330°C; thermogravimetric loss increased as temperature increased. However, when the temperature increased to over 450°C, the percentage of thermogravimetric loss was nearly 50%, which then stabilized with no further evidence of loss. That was because the PAN fibers had started carbonizing into carbon fiber. Additionally, it was also found (as shown in Figure 9) that PAN-COOH membrane, after it had already gone through the alkaline hydrolysis process, had a thermal decomposition pattern similar to that of unmodified PAN (its thermal decomposition temperature was about 320°C or so), confirming that it remained under appropriate conditional control. An alkaline hydrolysis reaction took place on the surface of PAN nanofiber membrane where it formed COOH functional groups, without destroying its internal bond, and the mechanical strength of the nanofibers was thereby maintained. Finally, the data showed that thermal stability of Sartobind® C membrane was not high. As the temperature increased, cracks in its structure (thermal decomposition temperature was approximately 115°C) occurred constantly, confirming that Sartobind® C was not suitable for high temperature operations. Neither was it able to perform high temperature sterilization, and its usage repetition was not high. Sartobind® C membrane was therefore limited in its application.

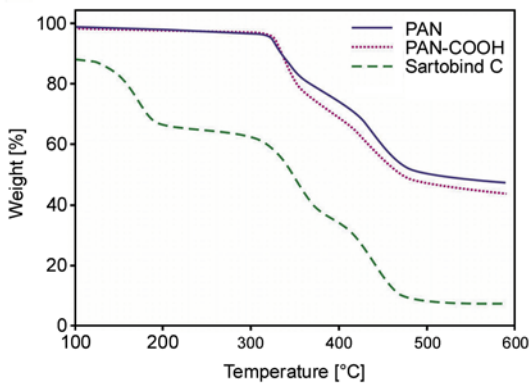

Figure 9. Thermogravimetric analysis of PAN, PAN-COOH, and Sartobind® C membranes

The morphology of the various nanofibrous membranes was examined by wide-angle X-ray diffraction (WXRD) as shown in Figure 10. The unmodi-

Table 1. Physical properties of different ion-exchange membranes

Membranes	Basis weight [g/m²]	Thickness [μm]	BET surface area [m²/g]	Porosity [%]	Ligand capacity [μeq/g]
Sartobind® C	128.04	261.2±7.6	0.8873	73.4	135.1
AEA-COOH	42.44	167.1±5.6	6.1768	84.4	439.8

PET: thickness 86.7 μm, basis weight 15 g/m^2

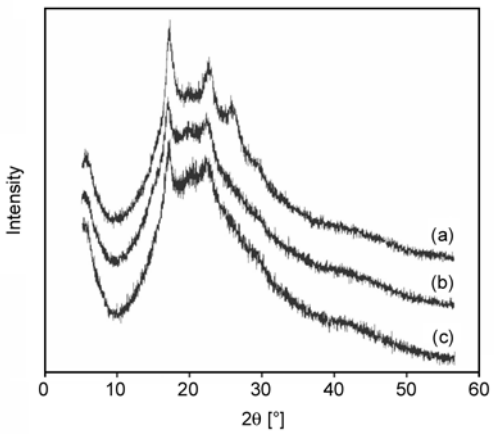

Figure 10. Wide-angle X-ray diffraction patterns of PAN nanofiber membranes at different alkaline hydrolysis conditions. (a) electrospun PAN nanofiber mat; (b) PAN-COOH at the alkaline hydrolysis condition of 85°C, 3N, 10 imn; (c) PAN-COOH at the alkaline hydrolysis condition of 85°C, 3N, 30 imn

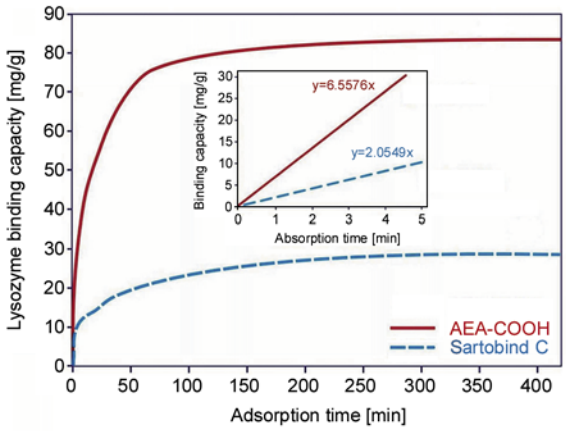

Figure 11. Lysozyme adsorption capacity on the (—)AEA-COOH and (– –) Sartobind® C. Temperature: 298 K; shaking rate: 150 rpm; adsorption solution: 0.5 mg/ml lysozyme in 20 mM glycine buffer (pH 9). The insert shows the initial linear adsorption rate.

fied PAN membrane exhibited three diffraction peaks at 17, 23, and 26°, which correspond to the crystalline structure of linear PAN. The diffractogram also showed peaks at 17 and 23° for PAN-COOH nanofibrous membranes under different alkaline hydrolysis conditions. The diffraction peak at 26º disappeared and only a minor decrease of relative intensity was observed when the PAN nanofibrous mat was modified with NaOH to substitute the nitrile groups with anion carboxylic acid groups, indicating minor interference of the crystalline formation for PAN-COOH. Combining TGA thermal stability data in Figure 9 with XRD results in Figure 10, this study confirmed that the rapid alkaline hydrolysis process only formed COOH functional groups on the surface of the PAN nanofiber membrane while under appropriate conditional control; the process did not cause any damage to its main structure. Thus, the PAN nanofiber membrane maintained a certain degree of mechanical integrity while simultaneously maintaining high-density ion functional groups.

3.4. Adsorption behavior of different ion-exchange membranes

Figure 11 shows comparisons of ion exchange membranes and their lysozyme adsorption volume. The results indicated that, using unit weight of membrane as a benchmark, under the adsorption conditions set with temperature of 298 K, stirring speed of 150 rpm, and lysozyme initial concentration of 0.5 mg/ml (in 20 mM glycine buffer (pH 9)), the maximum lysozyme adsorption capacity of Sartobind® C membrane was 28.6 mg/g. The AEA-COOH membrane was 83.2 mg/g, or about 2.9 times that of the commercial product. Under condition of fixed lysozyme concentration and adsorption time, comparison could be made on the adsorption rate among different ion exchange membranes, due to its initial linear absorption characteristic. Results of the experiment showed that the adsorption rate of AEA-COOH> Sartobind® C. Nanofiber structure based ion exchange membrane had an adsorption time 3.2 times faster than that of the commercial product.

4. Conclusions

This study combines electrospinning and alkali hydrolysis processes to create a weak acid ion exchange membrane possessing high surface functional group density, high porosity, and 3D nanofiber structure. The membrane facilitated an increase in lysozyme adsorption, improved fluid throughput, reduced pressure loss, enhanced overall efficiency of lysozyme purification, increased membrane life span, and reduced the cost of the adsorption membrane. Therefore, compared with the commercially available ion exchange membranes, the AEA-COOH nanofiber membrane was lighter and thinner, with a high adsorption capacity. It also had other unique characteristics such as low-pressure

drop and rapid adsorption rate. Its functional group density adjusted to changes in the duration of basic hydrolysis. It simultaneously possessed capabilities such as adsorption, micro-filtration, and bacteria filtration functions. During ion exchange, it can also filter out bacteria and small particles in order to reduce subsequent processing steps and overall purification time.

References

[1] An H., Shin C., Chase G. G.: Ion exchanger using electrospun polystyrene nanofibers. Journal of Membrane Science, **283**, 84–87 (2006).
DOI: 10.1016/j.memsci.2006.06.014

[2] Dominguez L., Benak K. R., Economy J.: Design of high efficiency polymeric cation exchange fibers. Polymers for Advanced Technologies, **12**, 197–205 (2001).
DOI: 10.1002/pat.125

[3] Kariduraganavar M. Y., Nagarale R. K., Kittur A. A., Kulkarni S. S.: Ion-exchange membranes: Preparative methods for electrodialysis and fuel cell applications. Desalination, **197**, 225–246 (2006).
DOI: 10.1016/j.desal.2006.01.019

[4] Kumar A., Gurian P. L., Bucciarelli-Tieger R. H., Mitchell-Blackwood J.: Iron oxide – Coated fibrous sorbents for arsenic removal. Journal of the American Water Works Association, **100**, 151–164 (2008).

[5] Greenleaf J. E., SenGupta A. K.: Environmentally benign hardness removal using ion-exchange fibers and snowmelt. Environmental Science and Technology, **40**, 370–376 (2006).
DOI: 10.1021/es051702x

[6] Ma Z., Lan Z., Matsuura T., Ramakrishna S.: Electrospun polyethersulfone affinity membrane: Membrane preparation and performance evaluation. Journal of Chromatography B, **877**, 3686–3694 (2009).
DOI: 10.1016/j.jchromb.2009.09.019

[7] Ding Z. J., Qi L., Ye J. Z.: Research on preparation of sheath-core bicomponent composite ion exchange fibers and absorption properties to metal ion. Macromolecular Research, **16**, 21–30 (2008).

[8] Stanelle R. D., Straut C. M., Marcus R. K.: Nylon-6 capillary-channeled polymer fibers as a stationary phase for the mixed-mode ion exchange/reversed-phase chromatography separation of proteins. Journal of Chromatographic Science, **45**, 415–421 (2007).

[9] Greenleaf J. E., Lin J-C., Sengupta A. K.: Two novel applications of ion exchange fibers: Arsenic removal and chemical-free softening of hard water. Environmental Progress, **25**, 300–311 (2006).
DOI: 10.1002/ep.10163

[10] Matsumoto H., Wakamatsu Y., Minagawa M., Tanioka A.: Preparation of ion-exchange fiber fabrics by electrospray deposition. Journal of Colloid and Interface Science, **293**, 143–150 (2006).
DOI: 10.1016/j.jcis.2005.06.022

[11] Wakamatsu Y., Matsumoto H., Minagawa M., Tanioka A.: Effect of ion-exchange nanofiber fabrics on water splitting in bipolar membrane. Journal of Colloid and Interface Science, **300**, 442–445 (2006).
DOI: 10.1016/j.jcis.2006.03.077

[12] Park S. A., Park K., Yoon H., Son J. G., Min T., Kim G-H.: Apparatus for preparing electrospun nanofibers: Designing an electrospinning process for nanofiber fabrication. Polymer International, **56**, 1361–1366 (2007).
DOI: 10.1002/pi.2345

[13] Barhate R. S., Ramakrishna S.: Nanofibrous filtering media: Filtration problems and solutions from tiny materials. Journal of Membrane Science, **296**, 1–8 (2007).
DOI: 10.1016/j.memsci.2007.03.038

[14] Teo W. E., Ramakrishna S.: A review on electrospinning design and nanofibre assemblies. Nanotechnology, **17**, 89–106 (2006).
DOI: 10.1088/0957-4484/17/14/R01

[15] Subbiah T., Bhat G. S., Tock R. W., Parameswaran S., Ramkumar S. S.: Electrospinning of nanofibers. Journal of Applied Polymer Science, **96**, 557–569 (2005).
DOI: 10.1002/app.21481

[16] Huang Z-M., Zhang Y-Z., Kotaki M., Ramakrishna S.: A review on polymer nanofibers by electrospinning and their applications in nanocomposites. Composites Science and Technology, **63**, 2223–2253 (2003).
DOI: 10.1016/S0266-3538(03)00178-7

[17] Frenot A., Chronakis I. S.: Polymer nanofibers assembled by electrospinning. Current Opinion in Colloid and Interface Science, **8**, 64–75 (2003).
DOI: 10.1016/S1359-0294(03)00004-9

[18] Ma Z., Ramakrishna S.: Electrospun regenerated cellulose nanofiber affinity membrane functionalized with protein A/G for IgG purification. Journal of Membrane Science, **319**, 23–28 (2008).
DOI: 10.1016/j.memsci.2008.03.045

[19] Dhanalakshmi M., Jog J. P.: Preparation and characterization of electrospun fibers of Nylon 11. Express Polymer Letters, **2**, 540–545 (2008).
DOI: 10.3144/expresspolymlett.2008.65

[20] Demir M. M.: Investigation on glassy skin formation of porous polystyrene fibers electrospun from DMF. Express Polymer Letters, **4**, 2–8 (2010).
DOI: 10.3144/expresspolymlett.2010.2

[21] Jayakumar R., Prabaharan M., Nair S. V., Tamura H.: Novel chitin and chitosan nanofibers in biomedical applications. Biotechnology Advances, **28**, 142–150 (2010).
DOI: 10.1016/j.biotechadv.2009.11.001

[22] Heikkliä P., Harlin A.: Electrospinning of polyacrylonitrile (PAN) solution: Effect of conductive additive and filler on the process. Express Polymer Letters, **3**, 437–445 (2009).
DOI: 10.3144/expresspolymlett.2009.53

[23] Chang Z. J., Zhao X., Zhang Q. H., Chen D. J.: Nanofibre-assisted alignment of carbon nanotubes in macroscopic polymer matrix via a scaffold-based method. Express Polymer Letters, **4**, 47–53 (2010). DOI: 10.3144/expresspolymlett.2010.8

[24] Li S-F., Chen J-P., Wu W-T.: Electrospun polyacrylonitrile nanofibrous membranes for lipase immobilization. Journal of Molecular Catalysis B: Enzimatic, **47**, 117–124 (2007). DOI: 10.1016/j.molcatb.2007.04.010

[25] Wang T., Kumar S.: Electrospinning of polyacrylonitrile nanofibers. Journal of Applied Polymer Science, **102**, 1023–1029 (2006). DOI: 10.1002/app.24123

[26] Yoon K., Kim K., Wang X., Fang D., Hsiao B. S., Chu B.: High flux ultrafiltration membranes based on electrospun nanofibrous PAN scaffolds and chitosan coating. Polymer, **47**, 2434–2441 (2006). DOI: 10.1016/j.polymer.2006.01.042

[27] Wang Z-G., Wan L-S., Xu Z-K.: Surface engineerings of polyacrylonitrile-based asymmetric membranes towards biomedical applications: An overview. Journal of Membrane Science, **304**, 8–23 (2007). DOI: 10.1016/j.memsci.2007.05.012

[28] Shunkevich A. A., Akulich Z. I., Mediak G. V., Soldatov V. S.: Acid-base properties of ion exchangers. III. Anion exchangers on the basis of polyacrylonitrile fiber. Reactive and Functional Polymers, **63**, 27–34 (2005). DOI: 10.1016/j.reactfunctpolym.2005.02.002

[29] Dai Z-W., Nie F-Q., Xu Z-K.: Acrylonitrile-based copolymer membranes containing reactive groups: Fabrication dual-layer biomimetic membranes by the immobilization of biomacromolecules. Journal of Membrane Science, **264**, 20–26 (2005). DOI: 10.1016/j.memsci.2005.04.022

[30] Yang M-C., Lin W-C.: Surface modification and blood compatibility of polyacrylonitrile membrane with immobilized chitosan-heparin conjugate. Journal of Polymer Research, **9**, 201–206 (2002). DOI: 10.1023/A:1021347810130

[31] Lin W-C., Liu T-Y., Yang M-C.: Hemocompatibility of polyacrylonitrile dialysis membrane immobilized with chitosan and heparin conjugate. Biomaterials, **25**, 1947–1957 (2004). DOI: 10.1016/j.biomaterials.2003.08.027

[32] Sasai Y., Matsuzaki N., Kondo S-I., Kuzuya M.: Introduction of carboxyl group onto polystyrene surface using plasma techniques. Surface and Coatings Technology, **202**, 5724–5727 (2008). DOI: 10.1016/j.surfcoat.2008.06.085